REPORT DOCUMENTATION PAGE

Form Approved
OMB No. 0704-0188

1. REPORT DATE *(DD-MM-YYYY)*
13-04-2009

2. REPORT TYPE
Journal Article

3. DATES COVERED *(From - To)*

4. TITLE AND SUBTITLE

Photothermal Deoxygenation of Graphene Oxide to Graphitic Carbon for Distributed Ignition and Patterning Applications (Postprint)

5a. CONTRACT NUMBER

5b. GRANT NUMBER

5c. PROGRAM ELEMENT NUMBER

6. AUTHOR(S)
Scott Gilje & Jabarri Farrar (Northrop Grumman); Sergey Dubin & Richard B. Kaner (UCLA); Alireza Badakshan (Sverdrup); S.A. Danczyk (AFRL/RZSA)

5d. PROJECT NUMBER

5e. TASK NUMBER

5f. WORK UNIT NUMBER
43470876

7. PERFORMING ORGANIZATION NAME(S) AND ADDRESS(ES)

Air Force Research Laboratory (AFMC)
AFRL/RZSA
10 E. Saturn Blvd.
Edwards AFB CA 93524-7680

8. PERFORMING ORGANIZATION REPORT NUMBER

AFRL-RZ-ED-JA-2009-152

9. SPONSORING / MONITORING AGENCY NAME(S) AND ADDRESS(ES)

Air Force Research Laboratory (AFMC)
AFRL/RZS
5 Pollux Drive
Edwards AFB CA 93524-7048

10. SPONSOR/MONITOR'S ACRONYM(S)

11. SPONSOR/MONITOR'S NUMBER(S)
AFRL-RZ-ED-JA-2009-152

12. DISTRIBUTION / AVAILABILITY STATEMENT

Approved for public release; distribution unlimited (PA #09227).

13. SUPPLEMENTARY NOTES
Published in Advanced Materials, **2010**, 22, 419-423. © 2010 WILEY-VCH Verlag GmbH & Co., KGaA, Weinheim

14. ABSTRACT

In recent years, several researchers have reported on an enhanced photothermal effect exhibited when nanoscale materials such as carbon nanotubes, polyaniline nanofibers or Si nanowires were irradiated using a photographic flash. **[1-3]**. In these studies, the high surface to volume ratio of the nanomaterials being flashed, coupled with the inability of the small structures to efficiently dissipate the absorbed energy, led to a rapid increase in temperature and subsequent ignition/welding of the materials. Although heating materials through the use of light energy is not a new phenomenon, achieving such a rapid and dramatic temperature change using only millisecond pulses of light demonstrates a tangible and technologically significant capability, unique to nanoscale materials. **[4]** We have been able to achieve an enhanced photothermally activated reaction by exposing nanostructured graphene oxide (GO) porous networks, to a photographic flash. The exposure results in a pronounced photoacoustic effect along with a rapid temperature increase, which initiates a secondary deoxygenation reaction to yield graphitic carbon and CO_2. A photo-initiated reaction could be used to achieve multiple ignition nucleation sites simultaneously. This type of "distributed ignition" has applications in liquid fuel rocket engines and in high efficiency homogenous charge compression ignition (HCCI) engines, where ignition control is of paramount importance.

15. SUBJECT TERMS

16. SECURITY CLASSIFICATION OF:			**17. LIMITATION OF ABSTRACT**	**18. NUMBER OF PAGES**	**19a. NAME OF RESPONSIBLE PERSON** Dr. S.A. Danczyk
a. REPORT **Unclassified**	**b. ABSTRACT** **Unclassified**	**c. THIS PAGE** **Unclassified**	SAR	6	**19b. TELEPHONE NUMBER** *(include area code)* N/A

Standard Form 298 (Rev. 8-98)
Prescribed by ANSI Std. 239.18

Photothermal Deoxygenation of Graphene Oxide for Patterning and Distributed Ignition Applications

By *Scott Gilje,** *Sergey Dubin*, *Alireza Badakhshan*, *Jabari Farrar*, *Stephen. A. Danczyk*, and *Richard B. Kaner*

A xenon discharge tube, such as is used to produce a photographic flash, has been reported to cause the ignition of carbon nanotubes, silicon nanowires, and welding of nanofibers of the conducting polymer polyaniline.[1–3] In these reactions, the high surface-to-volume ratio of the nanomaterials being irradiated, coupled with the inability of the small structures to efficiently dissipate the absorbed energy, leads to a rapid increase in temperature and subsequent ignition or welding of the materials. Although heating materials through the use of light energy is not a new phenomenon, achieving such a rapid and dramatic temperature change using only millisecond pulses of light demonstrates a tangible and technologically significant capability that is unique to nanoscale materials.[4]

Graphene oxide (GO) is a deeply colored, water dispersible, oxidized form of graphene obtained through the treatment of graphite powder with powerful oxidizing agents.[5] Although GO has been known for over 150 years, only recently have scientists had access to the tools necessary to properly analyze its atomically thin sheet structure. This has rekindled interest in graphite oxide and has led to a number of recent discoveries, including: the stacking of GO platelets to form paper-like materials of high modulus and strength.[6,7] Many studies have suggested that GO can be reduced to graphene-like carbon sheets by applying chemical reducing agents or by using thermal treatments.[8–10] This has led to speculation that GO could find use as a precursor in a bulk route to dispersible graphene sheets.[11–13] Already, several groups have succeeded in creating conducting polymer composites, transparent conducting films, and simple electronic devices based on reduced GO.[14–26] In addition to the chemical reduction of GO, Aksay, et al. have reported the thermal deoxygenation of GO to create functionalized graphene sheets upon rapid heating to 1100 °C under an inert atmosphere.[27,28] These organic solvent dispersible sheets have enabled the direct creation of polymer composites, without the need for surfactants.[29] Thermal deoxygenation of GO to form graphitic carbon dates back to the 1960s when Boehm and Scholz first reported on the ignition and deflagration of graphite oxides prepared by different methods.[30] Upon rapid heating to temperatures of ~200 °C, GO decomposes to the most thermodynamically stable oxide of carbon, CO_2. Along with the exothermic release of CO_2, H_2O, and CO also form as minor products.[31]

Carbon nanotubes have been considered as additives to rocket fuels to attain distributed fuel ignition because of the dramatic temperature increase (in excess of 1500 °C) that can be achieved using millisecond pulses of light. If different parts of the fuel can be ignited simultaneously, better control and stability along with lowered weight should be achievable.[32–34] Attempts aimed at using CNTs for ignition applications, however, have failed, since the CNT combustion requires outside oxygen. In fact, the CNTs themselves – like C_{60} and carbon soot – play little role in the ignition process, instead it is the iron nanoparticle catalyst used to grow them, along with oxygen, that supports combustion.[35–37] Even with sufficient catalyst, uniformly dispersing CNTs into liquid fuels remains problematic. Here we report the discovery of the photothermally initiated deflagration of GO that can take place even in an oxygen deficient environment. Since GO readily disperses in alcohols and other polar organic solvents, preliminary results indicate that with some chemical modification GO could be dispersed in fuels as well. This along with the current interest in GO as a nanoscale platelet material gave us the impetus to investigate this photothermally driven process further.

A random porous network of GO platelets is created by freeze-drying GO dispersions. The porous structure results from the extraction of water without causing collapse of the solid matrix of GO platelets due to capillary action, as would happen with conventional evaporation. Creating dry, low-density networks of nanoscale GO platelets serves two purposes: first, the surface to volume ratio of the platelets is increased providing maximum surface area for energy absorption; second, thermally conductive pathways through which absorbed energy can diffuse are reduced. The GO dispersions were comprised of platelets ranging in size from 100 nm–5 μm in diameter with the majority of platelets around 500 nm in diameter as analyzed by atomic force microscopy. The GO foam networks enable greater energy absorption and confinement leading to dramatic temperature increases on exposure to a camera flash. Using freeze-drying, porous GO foams can be made to densities down to 5 mg cm^{-3}

---

[*] Dr. S. Gilje, Dr. J. Farrar
Northrop Grumman Aerospace Research Labs
Northrop Grumman Corporation
Redondo Beach, California, 90278 (USA)
E-mail: scottgilje@yahoo.com

S. Dubin, Prof. R. B. Kaner
Department of Chemistry and Biochemistry and California NanoSystems Institute, University of California Los Angeles
Los Angeles, California, 90095 (USA)

Dr. A. Badakhshan
Jacobs Technology/Ross Group Air Force
Research Lab Edwards AFB, CA 93524 (USA)

Dr. S. A. Danczyk
AeroPhysics Branch, Combustion Devices Group
Air Force Research Laboratory; Edwards AFB, California (USA)

DOI: 10.1002/adma.200901902

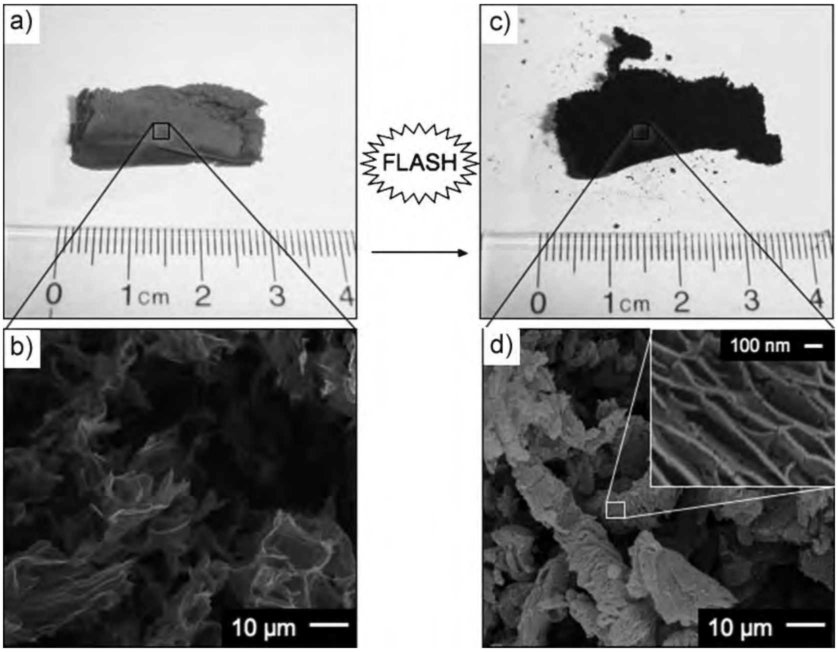

Figure 1. a) An image of a GO foam sample before exposure to a photographic flash. b) A scanning electron micrograph (SEM) shows the porous nature of the GO foam. c) After flashing, the GO foam ignites releasing CO_2 and H_2O and leaving behind an exfoliated, deoxygenated graphitic carbon. d) An SEM image of the material shows exfoliated layers. (inset) Under high magnification, the layers measure 10–20 nm in thickness.

before the structure collapses under its own weight. Most of the GO foams used in this study had a density of 15 mg cm^{-3}. Figure 1a is a photograph of a light-brown GO foam sample prepared by freeze drying a 15 mg ml^{-1} dispersion to achieve a density of 15 mg cm^{-3}. Figure 1b shows an SEM micrograph of the same sample magnified 1000×. In the SEM image, the GO platelets appear as crumpled sheets ranging in diameter from 500 nm to 20 μm, that assemble to form a porous three-dimensional network. The mechanical integrity of the GO foams increase with increasing density. Foams with a density of <5 mg cm^{-3} typically collapsed easily and were difficult to handle. Foams with a density ranging from 10 to 20 mg cm^{-3} were robust but required careful handling, while denser foams were quite sturdy much like a commercial silica aerogel. After flashing, the foams lose their structural robustness, fall apart, and are easily blown around by gusts of air.

Upon exposure to a photographic flash, the GO foam emits a popping sound most likely attributable to a photoacoustic effect similar to the flashing of CNTs.[38] A color change from light brown to dark black can be seen immediately after exposure to the flash indicating conversion to deoxygenated graphitic carbon. A photograph of the flashed GO foam is shown in Figure 1c. The light brown spots around the periphery of the sample correspond to the unreacted regions at the edges of the sample as a result of cooling and expansion of the foam as the reaction front propagates. Figure 1d, shows an expanded structure much like that of exfoliated graphite and comparable to recent reports on thermally reduced GO.[27,28] The inset picture of Figure 1d shows the flashed GO foam at 100000× magnification. At this magnification, the expanded nature of the flash deoxygenated graphitic platelets can be observed. Using the scale bar as a gauge, the thickness of the thinnest expanded sheets can be seen to range from 10 to 20 nm.

X-ray powder diffraction of a compressed pellet of the reduced graphite oxide shows a broad, low-intensity peak centered at $2\theta = 26.4^\circ$ indicating that after deflagration the product is, in fact, graphitic in nature.[30] The broadness of the diffraction peak is most likely due to both the small crystalline domain sizes of the graphitic planes and the turbostratic nature of the expanded sheets. The deoxygenated carbon material that remains after photothermally induced deoxygenation was analyzed for its carbon and oxygen content using X-ray photoelectron spectroscopy (XPS) (see Supporting Information). The carbon content increases from 68.7% in the GO starting material, to 92.1%, while the oxygen content decreases from 29.3 to 7.7%. The remaining oxygen is most likely contained in residual functionalities (−COOH, −OH, etc.) due to incomplete deoxygenation. Resistivity measurements taken on the deoxygenated carbon resulted in a resistivity decrease from $9.98 \times 10^4\ \Omega \cdot \mathrm{cm}$ before flashing to $2.23\ \Omega \cdot \mathrm{cm}$ after photoinduced deoxygenation. The change in resistivity of over four orders of magnitude is consistent with other forms of reduced GO obtained by thermal means.[27,28]

Due to the expanded nature of the flashed GO foams, they were analyzed for surface area by measuring N_2 gas uptake using the Brunaur-Emmett-Teller (BET) analysis method. Before flashing, a GO foam with a density 15 mg cm^{-3} was measured to have a surface area of 6 m^2 g^{-1}. After flashing, the measured surface area yielded a range from 400 to 980 m^2 g^{-1}. We believe the large range in values can be attributed to difficulties in determining the sample weight and adsorbed water content. Exposure of the flashed, deoxygenated carbon to hydrogen was performed, resulting in an uptake of 0.5 wt % at 77 K.

In addition to GO foam materials, it is possible to make GO films which can be photothermally patterned. To accomplish this, thin GO films (<1 μm in thickness) were created by filtering a dilute GO dispersion through a 0.2 μm Nylon Millipore filter. Figure 2a shows optical microscope images of a copper transmission electron microscope (TEM) grid placed on top of a GO film while still attached to the Nylon filter. Using the TEM grid as a mask, the GO film was exposed to a flash at close range inducing deoxygenation to graphitic carbon. Figure 2b is an optical microscope image of the GO film after flashing. Looking at the image, defined regions of black (exposed) and brown (masked) can clearly be seen mimicking the TEM grid mask. SEM images of the masked film (Fig. 2c) show how the exposed regions on the GO film expand outward upon ignition by the flash. The release of CO_2 and H_2O during deflagration is likely the cause of the platelets pushing out from the surface of the film.

Another promising application for photothermally initiated reactions is as an ignition promoter for fuels. By dispersing GO

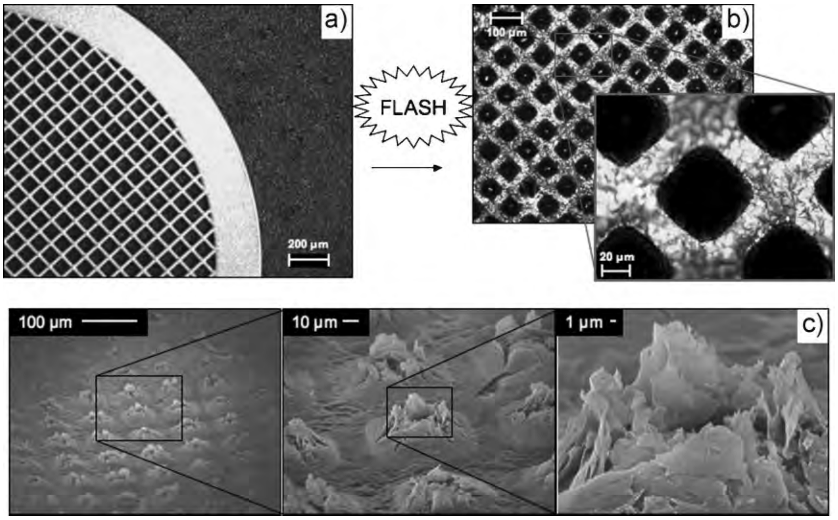

Figure 2. a) An optical microscopy image shows a GO film with a Cu transmission electron microscopy (TEM) grid on top before flashing. b) After flashing and removing the TEM mask, the pattern of the TEM grid has been transferred to the GO film as seen in the optical microscope images. c) The deoxygenation and subsequent release of CO_2 and H_2O blow the platelets of deoxygenated carbon out from the surface as depicted in series of SEM images at progressively higher magnifications.

platelets in a liquid fuel, it could be possible to initiate ignition of the fuel using a flash of light as opposed to a traditional spark plug. Illumination of a fuel/oxidizer mixture would enhance combustion by allowing ignition to occur at numerous locations simultaneously. One of the major drawbacks of current electrical spark ignition is that it is a single-point ignition source. Ideally, multiple ignition nucleation sites will allow for more controllable, and therefore more efficient and reliable ignition and combustion. This is of critical importance for applications such as liquid fueled rockets, where current ignition methods are known to be plagued by several problems. Issues such as combustion instability and start-up transients not only can cause severe damage, but also degradation in engine efficiency and an increase in emissions of pollutants. It is thought that nearly 30% of the combustion instabilities in rocket engines, leading to engine damage and possible loss of cargo and human life, can be traced back to the nature of the propellant's initial energy release process, as described by Harrje and Reardon.[39]

The short-comings of the existing systems combined with intuitive engineering advantages of low-energy, lightweight distributed ignition, has motivated previous attempts to use single wall carbon nanotubes (SWNTs) as photoignition enabling additives to fuels.[32–34] In these experiments, the SWNTs were found to only ignite in the presence of ambient oxygen and did not disperse well in the test fuels. Flashing of SWNTs is also heavily dependent on the Fe catalyst concentration. In contrast, GO carries its own oxygen supply and is highly dispersible in fuels such as alcohol; therefore, GO may be a promising additive as an ignition promoter for fuels.

In preliminary experiments, we have been able to successfully ignite ethanol fuels using GO as a photothermal initiator. Figure 3a shows a photo of a GO foam sample placed on a paper soaked with ethanol. Upon flashing (Fig. 3b), the ethanol vapor readily combusts as a result of the GO ignition. After the ethanol fuel is consumed, we can see the deoxygenated carbon product glowing bright red as a result of the combustion reaction and the volume of the sample increases due to exfoliation (Fig. 3c). Pyrometer readings of this ignition process indicate that by flashing GO achieves temperatures of 400–500 °C within a few ms. In our experiments, we were able to disperse GO platelets into ethanol and methanol with mild sonication. The GO platelets did not disperse well in more aliphatic fuels such as kerosene. We speculate that dispersibility of GO in organics could be facilitated with the use of surfactants without loss of the photothermal function of GO platelets as an ignition promoter.

Over the past decade, extraordinary efforts have been undertaken to both improve the fuel efficiency of traditional gasoline engines and search for clean, renewable alternative fuels to gasoline. One idea that has surfaced from this thrust is the notion of a homogeneous charge compression ignition (HCCI) engine that combines the high efficiency of a diesel engine with the low emissions of a spark ignition engine. In a typical HCCI engine, fuel and air are mixed homogeneously like a spark ignition engine, but ignition occurs by means of auto-ignition under high compression similar to a diesel engine.[40] The high compression ratio of HCCI engines provides an efficiency increase of up to 15% over traditional spark ignition engines.[41,42] Currently, one of the major challenges facing HCCI engines has been controlling the unpredictable compression-induced ignition process. By using an ignition promoter such as GO, it could be possible to achieve distributed ignition in HCCI engines, thus providing accurate ignition timing, resulting in the homogeneous detonation of fuel and air.

Highly absorbing nanoparticulate materials are able to achieve a dramatic temperature increase upon exposure to short pulses of moderate intensity light. These temperature increases occur as a

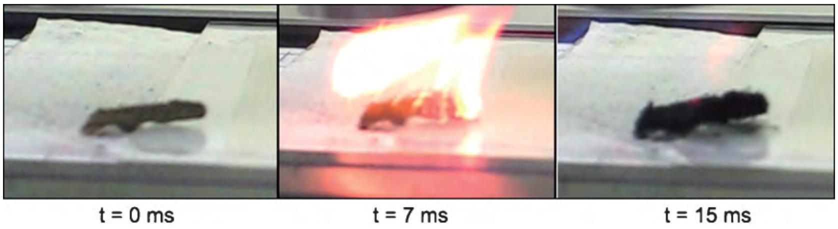

Figure 3. A series of photographs showing a GO foam sample before, during and after flash ignition with the time interval labeled in milliseconds (ms). By placing a GO foam sample onto a paper soaked with ethanol and flashing, the GO foam is capable of igniting the ethanol vapor as depicted in the center photograph. After ignition, the deoxygenated GO sample can be seen glowing red from the energy released during the reaction.

consequence of the high surface to volume ratio and low number of thermally conducting pathways by which to dissipate absorbed light energy. One of the distinguishing characteristics that sets photothermal ignition of GO apart from the flashing of other nanomaterials, is that instead of merely igniting or melting a material, an exothermic decomposition reaction occurs. The benefit of such a process is that the energy required for ignition is not provided solely by the source of the flash as it would be with other nanomaterials. This enables the use of lower power light sources and/or larger particles in order to achieve ignition, since the combustion of the particles themselves adds energy to the system. In the future, GO or other oxygen bearing, self-decomposing particles may make it possible to tune the photoignition behavior of a fuel to provide more controllable distributed ignition. In patterning applications, the solubility differences between GO and deoxygenated graphitic carbon could be used to quickly separate exposed and masked regions of a thin GO film. Using an organic solvent, the broken-up flashed areas of a GO film could be washed away leaving the masked GO portions intact. Subsequent thermal or chemical reduction of the patterned GO films to conducting, reduced GO would make it possible to create highly conducting patterns.[43]

Experimental

Synthesis: Graphene oxide was synthesized using a modified Hummer's method as reported previously in ref. [14]. Dispersions of GO were freeze-dried using an FTS systems Dura-Stop μP Freeze-drying system. Dispersion concentrations of 30, 15, 7.5, and 3.25 mg ml^{-1} were freeze-dried resulting in porous GO materials with densities of 30, 15, 7.5, and 3.25 mg cm^{-3}, respectively. Figure S1 is an SEM image of the lowest density 3.25 mg cm^{-3} sample showing the network of thin platelets. Film samples of GO were obtained by filtration of a GO dispersion through a 0.22 μm Anapore filter for free-standing films, and a 0.2 μm Nylon Millipore filter for thin films that remained bound to the filter membrane for stability.

Characterization: X-ray diffraction (XRD) was carried out using a PANalytical XPert Pro diffractometer with Cu Kα radiation ($\lambda = 1.5418$ Å). Before taking X-ray scans the GO was dried for 48 h under vacuum at room temperature followed by 24 h under vacuum over P_2O_5 which acts as a drying agent. Powder X-ray diffraction can be used to verify that the oxidation reaction has reached completion since the introduction of oxygen moieties expands the interplanar galleries in graphite from 3.34 to ~6.9 Å. Our graphite oxide exhibits a characteristic peak at 12.75 degrees 2θ corresponding to the 002 interplanar spacing of 6.94 Å, while the most intense peak from the starting graphite at 26.4 degrees 2θ, corresponding to a d-spacing of 3.34 Å, is completely absent. The d-spacing of slightly >6.9 Å for the synthesized GO indicates that despite drying under vacuum for 24 h, some water has been absorbed by the GO.

The GO and reduced GO samples were inserted into the analysis chamber of a ThermoVG ESCALAB 250, X-ray photoelectron spectrometer. Spectra were obtained by irradiating the sample with a 320 μm diameter spot of monochromated aluminum Kα X-rays at 1486.6 electron Volts (eV) under ultrahigh vacuum conditions. The analysis consisted of acquiring 10–20 scans and signal averaging. The survey scans were acquired with a pass energy of 80 eV, and the high resolution scans were acquired with a pass energy of 20 eV. Low pressure gas adsorption isotherms were measured volumetrically on an Autosorb-1 analyzer (Quantachrome Instruments). Conductivity data were obtained using a Jandel RM3-AR resistivity tester using an applied current of 4.532 μA in combination with a four-point probe head. Optical microscope images were taken using a Zeiss AxioTech 100 reflected light microscope with Zeiss AxioCam MRc camera.

A liquid nitrogen bath (77 K) was used for N_2 and H_2 isotherm measurements. The N_2, H_2, and He gases used were UHP grade. For measurement of the apparent surface areas (SLang), the Langmuir method was applied using the adsorption branches of the N_2 isotherms assuming a N_2 cross-sectional area of 16.2 $Å^2$/molecule. The micropore volumes (*V*p) were determined using the Dubinin-Raduskavich (DR) transformed N_2 isotherms across the linear region of the low pressure data.

Acknowledgements

The authors thank Hsiao Hu Peng for use of his lab facilities and freeze-drying system; Christina Baker, Vincent Tung, Jonathan Wassei, and Henry Tran for their help in carrying out measurements and intellectual contributions; Yan Xu for help making optical measurements; Dr. Hiroyasu Furukawa for carrying out hydrogen absorption measurements; and Grant Umeda for his help with the BET measurements. Funding for this research has been provided by The Northrop Grumman Corporation, Aerospace Systems Division, Aerospace Research Labs (ARL) internal research and development (IRAD) fund with matching support from the University of California Discovery Program (RBK), the Focused Center Research Program Functional Engineered Nano Architectonics (FCRP/FENA) Center (RBK), and the Air Force Research Labs (AFRL) Nano Energetics Strategic Technology Teams (STT). Supporting Information is available online from Wiley InterScience or from the author.

Received: June 5, 2009
Published online: October 26, 2009

---

[1] P. M. Ajayan, G. Ramanath, M. Terrones, T. W. Ebbesen, *Science* **2002**, *297*, 192.
[2] J. Huang, R. B. Kaner, *Nat. Nanotechnol.* **2004**, *3*, 783.
[3] N. Wang, B. D. Yao, Y. F. Chan, X. Y. Zhang, *Nano Lett.* **2003**, *3*, 475.
[4] J. Ying, *Nanostructured Materials*, Academic Press, New York **2001**.
[5] B. Brodie, *Ann. Chim. Phys.* **1855**, *45*, 351.
[6] D. Dikin, S. Stankovich, E. J. Zimney, R. D. Piner, H. B. Dommett, G. Evmenenko, S. T. Nguyen, R. S. Ruoff, *Nature* **2007**, *448*, 457.
[7] S. Park, K. S. Lee, G. Bozoklu, W. Cai, S. Nguyen, R. S. Ruoff, *ACS Nano* **2008**, *2*, 572.
[8] S. Stankovich, D. A. Dikin, R. D. Piner, K. A. Kohlhaas, A. Kleinhammes, Y. Jia, Y. Wu, S. T. Nguyen, R. S. Ruoff, *Carbon* **2007**, *45*, 1558.
[9] S. Stankovich, R. D. Piner, X. Chen, N. Wu, S. T. Nguyen, R. S. Ruoff, *J. Mater. Chem.* **2006**, *16*, 155.
[10] U. Hofmann, A. Frenzel, *Kolloid Z* **1934**, *68*, 149.
[11] V. C. Tung, M. J. Allen, Y. Yang, R. B. Kaner, *Nat. Nano.* **2008**, *4*, 25.
[12] D. Li, M. B. Muller, S. Gilje, R. B. Kaner, G. G. Wallace, *Nat. Nano.* **2007**, *3*, 101.
[13] S. Park, J. An, R. D. Piner, I. Jung, D. Yang, A. Velamakanni, S. T. Nguyen, R. S. Ruoff, *Chem. Mater.* **2008**, *20*, 6592.
[14] S. Gilje, S. Han, M. S. Wang, K. L. Wang, R. B. Kaner, *Nano Lett.* **2007**, *7*, 3394.
[15] C. Gomez-Navarro, R. T. Weitz, A. M. Bittner, M. Scolari, A. Mews, M. Burghrd, K. Kern, *Nano Lett.* **2007**, *7*, 3499.
[16] S. Stankovich, D. A. Dikin, G. H. B. Dommett, K. M. Kohlhaas, E. J. Zimney, E. A. Stach, R. D. Piner, S. T. Nguyen, R. S. Ruoff, *Nature* **2006**, *442*, 282.
[17] S. Watcharotone, D. A. Dikin, S. Stankovich, R. Piner, I. Jung, G. H. B. Dommett, G. Evmenenko, S. E. Wu, S. F. Chen, C. P. Liu, S. T. Nguyen, R. S. Ruoff, *Nano Lett.* **2007**, *7*, 1888.
[18] H. Chen, M. B. Muller, K. J. Gilmore, G. G. Wallace, D. Li, *Adv. Mater.* **2008**, *20*, 3557.
[19] R. Arsat, M. Breedon, M. Shafiei, P. G. Spizziri, S. Gilje, R. B. Kaner, K. Kalantar-zadeh, W. Wlodarski, *Chem. Phys. Lett.* **2008**, *467*, 344.

[20] M. D. Stoller, S. Park, Y. Zhu, J. An, R. S. Ruoff, *Nano Lett.* **2008**, *8*, 3498.

[21] L. J. Cote, F. Kim, J. Huang, *J. Am. Chem. Soc.* **2009**, *101*, 1043.

[22] E. Goki, Y. Y. Lin, S. Miller, C. W. Chen, W. F. Su, M. Chhowalla, *Appl. Phys. Lett.* **2008**, *92*, 233305.

[23] X. Wang, L. Zhi, N. Tsao, Z. Tomovic, J. Li, K. Muller, *Angew. Chem. Int. Ed.* **2008**, *47*, 2990.

[24] J. Wu, H. A. Bercerril, Z. Bao, Z. Liu, Y. Chen, P. Peumans, *Appl. Phys. Lett.* **2008**, *92*, 263302.

[25] E. Goki, G. Fanchini, M. Chhowalla, *Nat. Nanotechnol.* **2008**, *3*, 270.

[26] X. L. Li, G. Zhang, X. Bai, X. Sun, X. Wang, E. Wang, H. Dai, *Nat. Nanotechnol.* **2008**, *3*, 538.

[27] H. C. Schneipp, J. L. Li, M. J. McAllister, H. Sai, M. Herrera-Alonso, D. H. Adamson, R. K. Prud'homme, R. Car, D. A. Saville, I. A. Aksay, *J. Phys. Chem. B.* **2006**, *110*, 8535.

[28] J. L. Li, K. N. Kudin, M. J. McAllister, R. K. Prud'homme, I. A. Aksay, R. Car, *Phys. Rev. Lett.* **2006**, *96*, 176101.

[29] T. Ramanathan, A. A. Abdala, S. Stankovich, D. A. Dikin, M. Herrera-Alonso, R. D. Piner, D. H. Adamson, H. C. Schniepp, X. Chen, R. S. Ruoff, S. T. Nguyen, I. A. Aksay, R. K. Prud'homme, L. C. Brinson, *Nat. Nanotechnol.* **2008**, *3*, 327.

[30] H. P. Boehm, W. Scholz, *Z. Anorg. Allg. Chem.* **1965**, *335*, 74.

[31] *Oligomerization and Polymerization Formation of Intercalation Compounds, Volume 17, Inorganic Reactions and Methods* (Eds: J. J. Zuckerman, A. P. Hagen), Wiley-VCH, New York **1990**.

[32] B. Chehroudi, S. A. Danczyk, presentation *Global Powertrain Congress—World Powertrain Exposition*, Novi, Michigan. September **2006**.

[33] S. Sciamanna, C. Munson, G. Dieckmann, *US Patent Application* #11/613105, **2006**.

[34] C. Beiver, *New Scientist Magazine* **2005**, *2526*, 30.

[35] N. Braidy, G. A. Botton, A. Adronov, *Nano Lett.* **2002**, *2*, 1277.

[36] J. Smits, B. Wincheski, M. Namkung, R. Crooks, R. Louise, *Mater. Sci. Eng. A* **2003**, *358*, 384.

[37] I. W. Chiang, B. E. Brinson, A. Y. Huang, P. A. Willis, M. J. Bronikowski, J. L. Margrave, E. R. Smalley, R. H. Hauge, *J. Phys. Chem. B.* **2001**, *105*, 8297.

[38] H. Chen, G. Diebold, *Science* **1995**, *270*, 963.

[39] D. T. Harrje, F. H. Reardon, *Liquid propellant rocket combustion instability, NASA SP-194, Scientific and Technical Information Office*, Washington, D.C. **1972**.

[40] B. Chehroudi, Homogeneous charge compression ignition (HCCI) engine, *Powertrain International* **2002**, *5*, 6.

[41] S. Magnus, J. E. Dec, N. P. Cernansky, *Soc. Automotive Eng.* **2005**, *1*, 0113.

[42] F. Zhao, *Homogeneous Charge Compression Ignition (HCCI) Engines: Key Research and Development Issues* (Eds: Thomas W. Asmus, Dennis N. Assanis, John E. Dec, James A. Eng, Paul M. Najt), Society of Automotive Engineers International, Warrendale, PA **2003**, pp. 11–12.

[43] At least a portion of the technology that is discussed in this paper is the subject of one or more pending patents.